JOURNAL OF GEOPHYSICAL RESEARCH, VOL. 111, A06307, doi:10.1029/2005JA011448, 2006

Day-to-day variability of the *E* layer

Luke Moore,[1] Michael Mendillo,[1] Carlos Martinis,[1] and Scott Bailey[2]

Received 28 September 2005; revised 6 March 2006; accepted 9 March 2006; published 22 June 2006.

[1] Noontime day-to-day variability of ionosonde and incoherent scatter radar (ISR) measurements of the *E* layer are analyzed for two time periods: 9–27 March 1999 and 4 October–4 November 2002. *E* layer variability is found to be between 5 and 7% at midlatitudes for these periods. Polar latitudes demonstrate variability ranging from ~7 to 50%, resulting primarily from a combination of photochemical and auroral processes. In order to understand the relative importance of the various sources that drive the variability in the *E* layer, a one-dimensional time-dependent photochemical model of the Earth's upper atmosphere is developed. The model is able to reproduce *E* layer electron density and variability for both time periods at a number of mid- and low-latitude stations. It is shown that *E* layer variability is dominated by variations in the incident solar flux for mid- and low-latitude stations, while auroral ionization processes are estimated to contribute roughly 30% of the total variability observed at polar stations. Changes in the solar declination over the time periods studied are responsible for a secondary source of *E* layer variability at midlatitudes and for a primary source at high latitudes. Day-to-day changes in neutral atmosphere species (including observed NO densities) contribute the least to overall *E* layer variations, except at low latitudes, where their contribution to variability is comparable to variability induced by changes in solar declination.

Citation: Moore, L., M. Mendillo, C. Martinis, and S. Bailey (2006), Day-to-day variability of the *E* layer, *J. Geophys. Res.*, *111*, A06307, doi:10.1029/2005JA011448.

1. Introduction

[2] The Earth's ionospheric *E* layer has historically been considered an ideal application of simple Chapman theory. It is a layer primarily in photochemical equilibrium, with short chemical loss time constants leading to relative isolation; yet, it is not in conformity with Chapman's formulation of a single constituent atmosphere ionized by a monochromatic photon flux. Further complications in bridging the gap between observations and theory include accurate knowledge of solar X-ray and EUV irradiance, neutral atmospheric abundances, and secondary ionization processes. With recent advances in these areas it is possible to construct a model of the *E* layer that is accurate under a variety of different geophysical conditions [e.g., *Buonsanto et al.*, 1992, 1995; *Titheridge*, 1996, 1997]. Such a model can be applied at any time and location, and can be used to study the day-to-day variability of the *E* layer. Understanding the variability of the Earth's primary photochemical ionospheric layer in detail is beneficial to the study of other photochemical layers in the solar system. Additionally, *E* layer conductivities (derived from electron and ion densities) play important roles in a host of ionospheric phenomena, ranging from the equatorial electrojet to magnetosphere-ionosphere coupling.

[3] The *E* layer is produced mainly from photoionization of molecular nitrogen (N_2) and oxygen (O_2); however, charge exchange processes lead to an ionosphere dominated by NO^+ and O_2^+. Neutral nitric oxide (NO) plays an important role by altering the ion photochemistry, and can additionally affect the thermal balance in the thermosphere by radiating in the infrared. Despite this importance, NO is a minor atmospheric constituent ($\sim 10^{-4}$ mixing ratio at the *E* layer peak) and had been observed and modeled infrequently by the aeronomy community prior to 1998. On 27 February 1998, the Student Nitric Oxide Explorer (SNOE [*Solomon et al.*, 1996]) was launched, and made global observations of NO as well as solar X-ray irradiance for nearly 6 years [*Barth et al.*, 2003]. A subsequent modeling study that used the NRLMSISE-00 model [*Picone et al.*, 2002] as a base and SNOE solar X-ray measurements as input demonstrated that thermospheric NO variability was driven by solar soft X rays at low latitudes [*Bailey et al.*, 2002; *Barth et al.*, 2004]. At high latitudes, auroral electron precipitation is a major source of NO [*Solomon et al.*, 1999; *Marsh et al.*, 2004]. The above conclusions agree qualitatively with previous studies [e.g., *Barth et al.*, 1988; *Siskind et al.*, 1989a, 1989b] based on the NO data sets of the 1980s and 1990s from the Solar Mesosphere Explorer (SME, 1982–1986) and the Halogen Occultation Experiment (HALOE, aboard the UARS satellite, 1992–1995) [*Russell et al.*, 1994; *Siskind et al.*, 1998].

[1] Center for Space Physics, Boston University, Boston, Massachusetts, USA.
[2] Geophysical Institute, University of Alaska Fairbanks, Fairbanks, Alaska, USA.

0148-0227/06/2005JA011448$09.00

Table 1. Modeled Sources of Noontime *E* Layer Variability[a]

			9–27 Mar 1999, %				4 Oct to 4 Nov 2002, %			
Station	Latitude, deg	Longitude, deg	A	B	C	D	A	B	C	D
Bermuda	32.0	−64.5	1.28	0.90	0.28	9.13	3.37	0.84	0.31	4.34
Dyess	32.4	−99.7	1.43	0.78	0.13	8.95	3.48	0.78	0.18	4.25
Eglin	30.4	−86.7	1.28	1.47	0.40	9.32	3.20	0.66	0.25	4.36
Jicamarca	−12.1	−77.0	0.54	1.22	0.43	7.84	0.44	0.48	0.38	4.60
Millstone Hill	42.6	−71.5	2.15	1.79	0.22	8.88	5.20	1.04	0.36	4.20
Svalbard	78.2	18.0	7.85	0.50	0.52	8.31	13.8	2.42	0.60	2.61
Tromso	69.7	19.0	6.84	1.50	1.27	9.22	20.1	0.93	0.31	3.91
Wallops	37.8	−75.5	1.76	1.41	0.16	8.97	4.23	0.99	0.25	4.26
Zhongshan	−69.4	76.4	6.26	2.44	0.26	8.52	6.21	0.47	0.39	4.21

[a]The values given represent the standard deviations about noontime NmE mean values for model calculations with one variable source: A, solar declination; B, NO density; C, neutral atmosphere, or D, solar flux. The three other sources are held constant in each case.

[4] Observations of NO are important for understanding *E* layer electron densities, as they remove one unknown from the study. If solar flux and neutral densities are known simultaneously, then any remaining discrepancy between predicted and measured electron density at noon can be attributed to uncertainties in the primary and secondary ionization processes. (Other ionization processes in the *E* layer, such as meteoric influx, contribute only a minor fraction of daytime electron density on average [*Grebowsky et al.*, 1998]). Complete calculations of photoelectron flux as a function of height and energy are quite complicated, and so ionospheric calculations typically parameterize the effect of secondary ionization [e.g., *Richards and Torr*, 1988; *Lilensten et al.*, 1989]. A recent *E* layer secondary ionization parameterization by *Titheridge* [1996] provides the advantage of subdividing secondary ionization rates by species and wavelength, and compares well with full photoelectron calculations, as well as electron density observations.

[5] This study investigates the sources of day-to-day variability in the *E* layer with a one-dimensional time-dependent photochemical model. By making use of the SNOE database of NO and the SOLAR2000 irradiance model, it is possible to separate sources of variability and to evaluate the performance of various parameterizations in the *E* layer. One such source, that of auroral ionization processes, is not modeled directly, but can be inferred from discrepancies between model and observations at polar latitudes.

2. Observations

[6] Ionospheric data used here come from two sources: ionosonde measurements of the *E* layer downloaded from the Space Physics Interactive Data Resource (SPIDR, http://spidr.ngdc.noaa.gov/spidr), and incoherent scatter radar (ISR) data retrieved from the Madrigal Database (http://www.openmadrigal.org). Ionosondes are operated more or less continuously at a number of stations distributed across the globe, making them excellent sources of data for day-to-day studies of the ionosphere. Unfortunately, f_oE, or the frequency at which an ionosonde's radio pulse is reflected by the *E* layer (and equal to the plasma frequency at that location), is usually determined to only 0.1 MHz precision, which corresponds to steps of order 10^4 electrons cm^{-3} in measured density. Ionosonde returns are not easily inverted to yield height profiles of electron density on a continuous basis, and thus it is their broad spatial contributions of f_oE data that are most important to this study.

[7] Incoherent scatter data are complimentary to ionosonde data in that they provide an altitude distribution of electron density that can be compared with model output, as

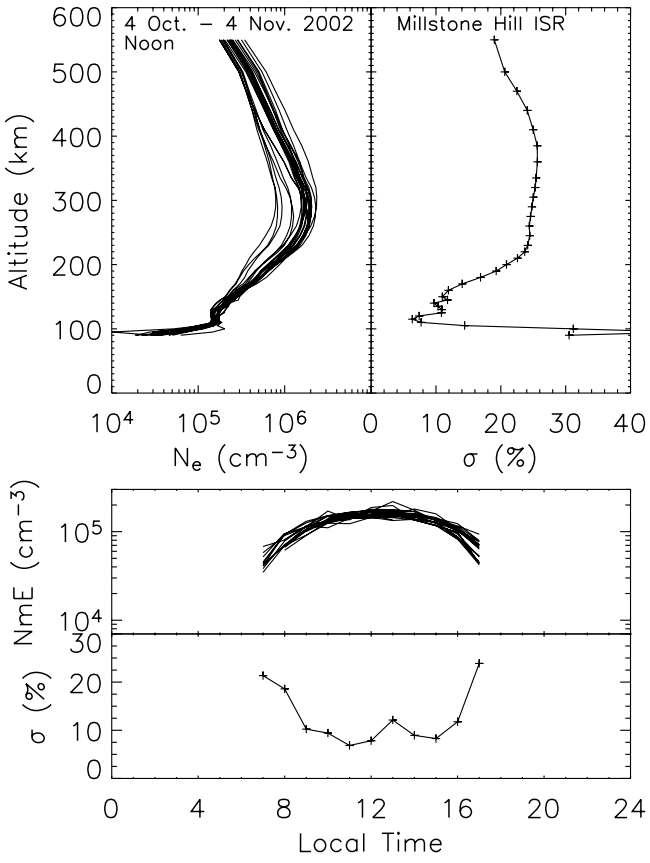

Figure 1. Incoherent scatter radar (ISR) measurements at Millstone Hill from 4 October to 4 November 2002. (top) Noontime electron density altitude profile for each of the 32 days during the period (left), along with the standard deviation about the sample mean (right). (bottom) Diurnal variation of peak *E* layer electron density, N_mE, for each day and the standard deviation in N_mE.

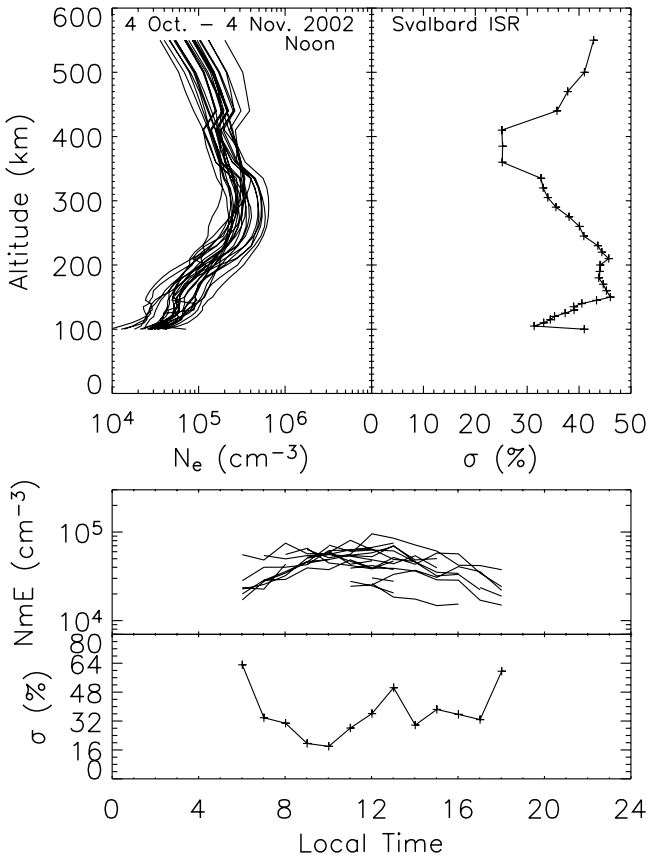

Figure 2. Same as Figure 1, but for the EISCAT Svalbard Radar.

well as a useful tool for diagnosing periods of unusual *E* layer electron densities (such as metallic ions from meteoric influx [*Grebowsky et al.*, 1998]). Incoherent scatter radars require large amounts of power, and have many other applications in addition to measuring vertical profiles of electron density; thus it is unusual to find a continuous ISR data set on which to base a study of day-to-day variability. However, from 4 October to 4 November 2002, the ISR facilities at Millstone Hill, Massachusetts, and Longyearbyen, Svalbard, conducted the "30-day Long Duration Experiment," which addressed this deficiency directly (see Table 1 for station details). For this period, ionosonde data were available from six stations with adequate coverage (i.e., measurements of *E* layer densities for most of these 32 days): Dyess, Eglin Air Force Base (AFB), Jicamarca, Millstone Hill, Tromso, and Wallops.

[8] As a continuation of a previous study of simultaneous ionospheric variability on Earth and Mars [*Mendillo et al.*, 2003; *Rishbeth and Mendillo*, 2004], the period of 9–27 March 1999 was also chosen, for which six ionospheric stations had good coverage: Bermuda, Eglin AFB, Jicamarca, Millstone Hill, Wallops, and Zhongshan. These two periods provide a basis for comparing ionospheric variability across time and space, and with different observing techniques, and will henceforth be referred to as the 1999 and the 2002 periods.

[9] Ionospheric data at SPIDR have already been scaled, and therefore the parameter f_oE is retrieved as a function of time, and converted into N_mE, or electron density at the peak of the *E* layer. Individual ionosonde values of N_mE versus local time were rejected when f_oE was constant for more than 4 hours during the day (a nonphysical situation); no more than 5 days from a period were rejected for a single station except for Jicamarca in 2002, where 14 days were rejected. Incoherent scatter radar data from the Madrigal Database are also reduced, but require some additional analysis in order to recast them into $N_mE(t)$. First, the electron density profiles are binned in altitude (variable grid size, 5 km at 90 km altitude, and 50 km at 600 km altitude) and time (1 hour). Next, an algorithm detects the location of the *E* layer by determining the local maximum between 100 and 120 km. (This technique works well during daytime hours, when the maximum is easily detectable, but scatter in the measurements and the lack of a clear peak between dusk and dawn make for larger uncertainty in N_mE during those hours.) The 2002 data from the Millstone Hill ISR and the EISCAT Svalbard Radar (ESR) are given in Figures 1 and 2, which display altitude profiles of electron density at 1200 LT, and the derived diurnal N_mE profile for the entire period of 32 days.

[10] An illustration of the ionosonde data for the same 2002 period is given in Figures 3 and 4. Figures 3a and 4a and Figures 3c and 4c show the diurnal variation of N_mE for each of the days studied at Millstone Hill and Eglin AFB, respectively. Beneath each of the scatter plots of N_mE is the standard deviation over the time period studied. These figures, and the modeling results shown in Figures 3c, 3d, 4c, and 4d, are described in more detail under section 4.

[11] Measurements of NO density come from the SNOE satellite. The NO measurements are given as a function of latitude, longitude, and altitude, and so no additional analysis was necessary. For the 1999 period, the NO data are spaced ~3 km in altitude (95–150 km range) and 5° in latitude. The NO data from the 2002 period have a vertical grid spanning 80–170 km, but are similar otherwise. Examples are shown for Millstone Hill in Figure 5 together with MSIS neutral atmosphere profiles for the major constituents throughout this period. The MSIS variability is typical of all locations used in this study. For the low- and mid-latitude stations, the variability in neutral NO at *E* layer altitudes were all similar (~20–30%), while polar latitudes stations showed significantly more NO variability (~50–60%).

3. Model

3.1. Photochemical Model Description

[12] A one-dimensional time-dependent photochemical model has been developed to study the day-to-day variability of the *E* layer. The modeling description is identical to that developed for the Martian ionosphere by *Martinis et al.* [2003], and as applied to the ionosphere of Saturn [*Moore et al.*, 2004]. A summary of that approach is given here.

[13] The model solves the one-dimensional ion continuity equations:

$$\frac{\partial n_i^+}{\partial t} = P_i - L_i, \tag{1}$$

where ion production ($P_i = A_i n_i$) can come from photoionization ($A_i = J_i$) or charge-exchange reactions

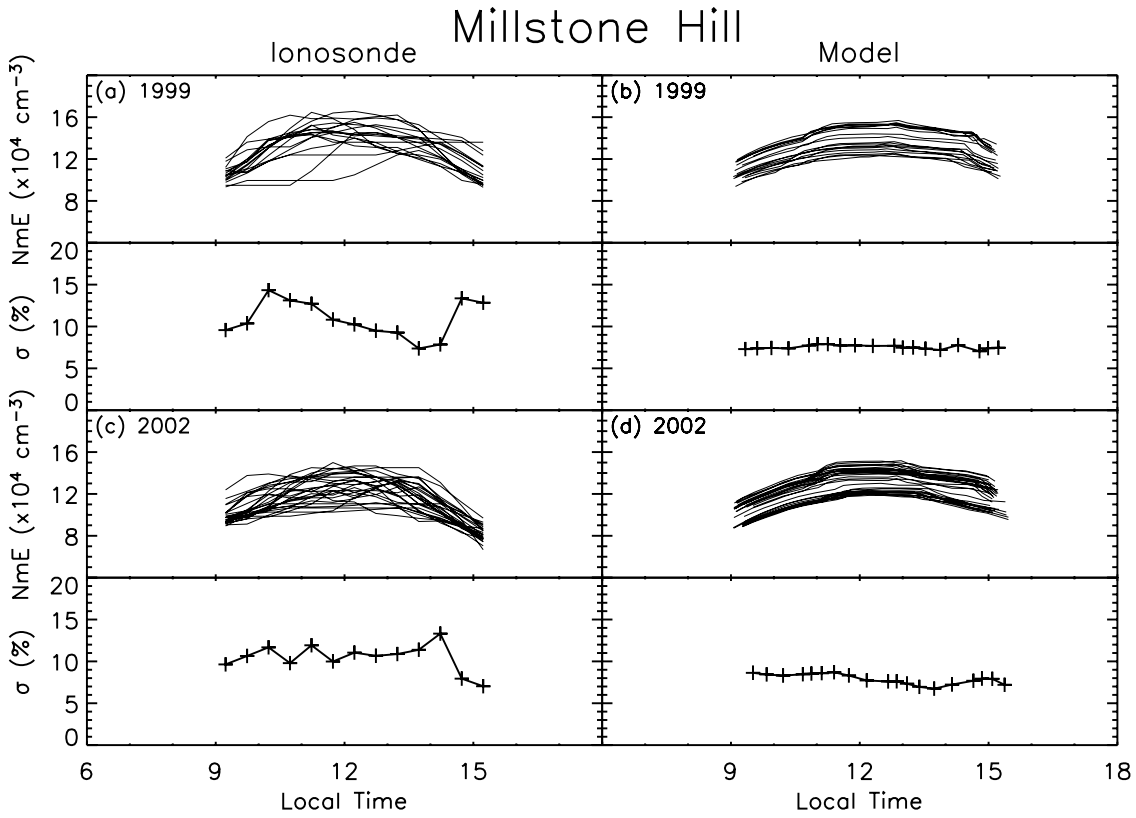

Figure 3. Comparison between modeled and measured (via ionosonde) *E* layer electron densities (N_mE) at Millstone Hill (42.6° latitude) for each time period, 9–27 March 1999 and 4 October–4 November 2002. Each profile in the top half of the separate panels represents the diurnal variation of N_mE over the course of one day; thus there are 19 profiles for the 1999 period and 32 profiles for the 2002 period. The profile in the bottom half of each panel grouping is the standard deviation about the mean for those 19 (or 32) days.

($A_i = k_{ij}n_j^+$), and ion loss ($L_i = B_i n_i^+$) is due either to recombination ($B_i = \alpha_i n_e$) or charge-exchange ($B_i = k_{ij}n_j$). Under this notation A_i and B_i are generic production and loss rates (s^{-1}) for the species n_i^+; J_i is the photoionization rate (s^{-1}) of n_i; k_{ij} is the rate coefficient for a charge-exchange reaction between n_i and n_j ($cm^3\ s^{-1}$); and α_i is the recombination coefficient for n_i^+ ($cm^3\ s^{-1}$). Electron density is taken to be the sum of the individual ion densities.

[14] Equation (1) then becomes a first-order linear differential equation, and can be solved when P_i and B_i are constant (which is valid for small time steps), giving

$$\Delta n_i^+ = \left(\frac{P_i}{B_i} - n_{i\,o}^+\right)\left(1 - e^{-B_i \Delta t}\right), \tag{2}$$

where Δn_i^+ is the change in density for the ith ion over a time interval Δt. The time steps are variable such that when the rate of change in ion density is largest (i.e., during dawn and dusk) the time steps are smallest. Typically, the time step will range from 1 μs to 100 ms over the course of a day. As the model does not include ion diffusion, it does not accurately predict electron densities in the upper ionosphere.

[15] To make the model Earth specific, the neutral atmosphere comes from NRLMSISE-00 [*Picone et al.*, 2002, and references therein], which is an empirical model spanning 0–1000 km altitude that provides estimates of neutral temperature, and N_2, O, O_2, He, Ar, and H densities. Solar irradiances come from the SOLAR2000 empirical model (v2.22) [*Tobiska et al.*, 2000; *Tobiska*, 2004], and span 10–1050 Å, as well as Lyman-α, which ionizes nitric oxide. These photons are attenuated through the neutral atmosphere using recent photoabsorption and photoionization cross sections; calculations of ion density (equation (2)) are made using the photochemistry described in Table 2 [*Schunk and Nagy*, 2000]. Ion, and thus electron (= sum of ions), altitude profiles are generated as functions of time, so the algorithm that was used to detect the peak *E* layer electron density in the ISR data is applied here as well, giving $N_mE(t)$.

3.2. Nonphotoionization Processes

[16] Secondary ionization production rates developed by *Titheridge* [1996] are adopted in this study, as they represent the most recent species-dependent rates, and they do not require full photoelectron transport calculations. Other secondary ionizations for the *E* layer in the literature include parameterizations by *Richards and Torr* [1988], and *Lilensten et al.* [1989], as well as a steady state two-stream calculation of photoelectron fluxes [*Solomon et al.*,

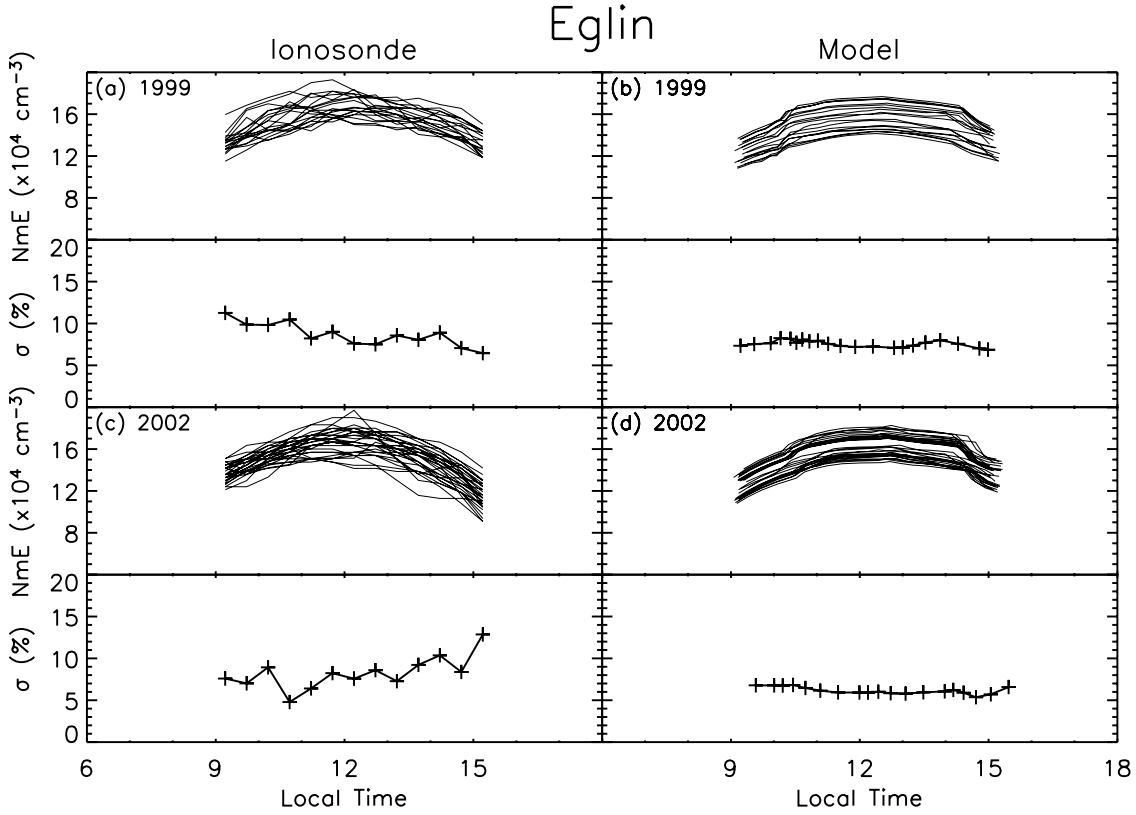

Figure 4. Same as Figure 3, but for Eglin Air Force Base (30.4° latitude).

1988; *Solomon and Abreu*, 1989]. A description of these methods for modeling photoelectron ionization is given by *Buonsanto et al.* [1992]. For his study, Titheridge used the EUVAC empirical model of solar irradiance [*Richards et al.*, 1994]. In this work, a more recent empirical model of solar irradiance, SOLAR2000 (v2.22), is used, as it is continually updated with new satellite measurements and it includes two additional wavelength bins representing soft X rays, which are important for *E* layer ionization.

[17] When the photochemical model described in section 3.1 was compared with observations (using SOLAR2000 v1.23, NRLMSISE-00, SNOE NO data, and the Titheridge secondary ionization rates) there was very good agreement; with the release of SOLAR2000 v2, however, the modeled *E* layer electron densities were consistently too low. Version 2 of SOLAR2000 incorporated newer measurements and calibrations, and differed from previous versions most notably by predicting different X-ray fluxes and a much smaller HeII flux (at 303.8 Å). The net effect of using v2 solar fluxes instead of the v1 solar fluxes was that modeled electron densities were smaller both at Saturn [*Moore et al.*, 2004] and in this study. By increasing the Titheridge parameterization by a factor of 2.2 across all wavelengths and species, the v2 model calculations were brought into agreement with v1 calculations, as well as observations. An increase in the Titheridge secondary ionization rates by a factor of 2.2 is equivalent to increasing the total ionization rate by a factor of ~2. This multiplicative factor of 2.2 might be viewed as a coupled uncertainty between the primary (i.e., solar flux, photoionization cross sections, and neutral atmosphere) and the secondary ionization rates rather than a "new" *E* layer parameterization. Certainly, this is a topic for which further research is necessary and justified, as well as validation studies for the various versions of SOLAR2000. The primary goal in this study is relative day-to-day change, and that can be assessed independently from such concerns.

[18] Auroral ionization processes are not included in the modeling. The model is shown below to yield good agreement with the observations at low and midlatitudes. Therefore the amount of ionization due to electron precipitation can be "measured" by the discrepancy between model and data at polar latitudes with fairly good confidence. This inferred ionization, and its effect on the overall variability of the *E* layer, can be quite significant, as discussed below in section 4.

3.3. Drivers of Variability

[19] Four sources of variability are identified and their effects modeled: (1) changes of solar declination over the time period studied, (2) NO density variations, (3) neutral atmospheric variations (i.e., all non-NO species), and (4) solar flux variations. In addition, variability due to auroral ionization processes is studied by making use of the fact that the photochemical model does not include these processes, and thus any disagreement between model and data in polar regions can be attributed to them. The change of solar declination is a purely geometrical effect that becomes more important at higher latitudes and also for longer time periods. Nitric oxide variations are evaluated separately from the rest of the neutral atmosphere because observations of NO are available while the rest of the

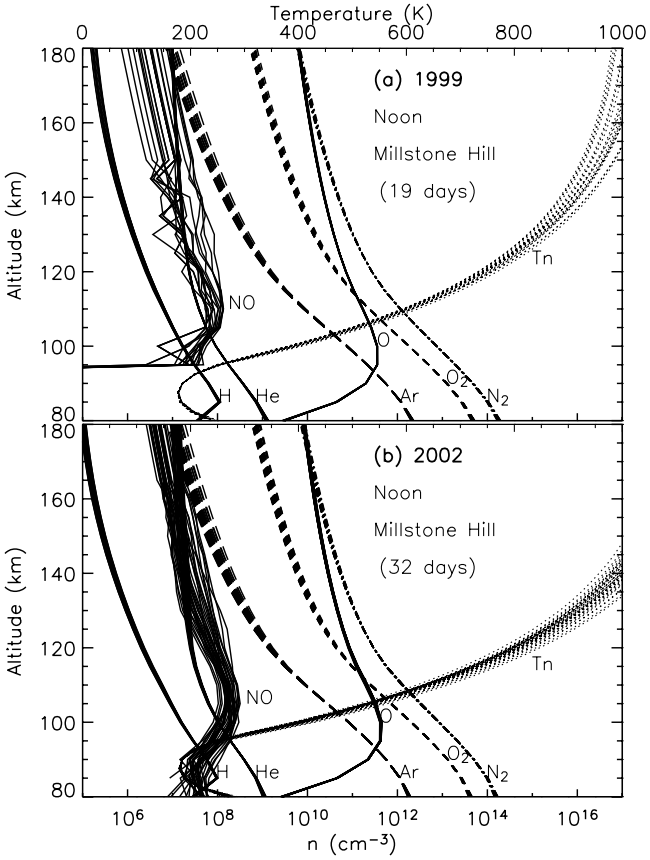

Figure 5. Neutral atmosphere obtained from NRLMSISE-00, including NO from the SNOE satellite. The NO density is extrapolated from the SNOE data based on the scale height of NO. Each noontime profile at Millstone Hill is overplotted for (a) 9–27 March 1999 and (b) 4 October–4 November 2002.

atmosphere must be modeled. In addition, there has been much discussion in the literature about the important role of NO in *E* layer photochemistry, and this study can provide a new outlook on that importance [e.g., *Solomon et al.*, 1996; *Titheridge*, 2000; *Marsh et al.*, 2004].

[20] As in any case study, the variability of the *E* layer for the two periods described above, 9–27 March 1999 and 4 October–4 November 2000, depends directly on the drivers of that variability, and so those sources are given in Figures 5 and 6. In Figure 5, the neutral atmospheres at noon for each of the 19 (1999) and 32 (2002) days are plotted on the same graph. There is little scatter present in the non-NO species, as they are modeled using NRLMSISE-00, while the NO is directly observed by SNOE and demonstrates larger variability. The solar declination change over the time periods studied was $\sim 7°$ for the 19 days in 1999 (spanning $-4.5°$ to $2.5°$) and $\sim 11°$ for the 32 days in 2002 (spanning $-4°$ to $-15°$). Finally, the solar inputs for the two periods are given in Figure 6. Figures 6a and 6b are the solar and geomagnetic input parameters that drive the NRLMSISE-00 model, while Figures 6c and 6d show the SOLAR2000 v2.22 photon flux as a function of wavelength over the portion of the spectrum responsible for photoionization in the *E* layer. An additional source of direct photoionization of NO is Lyman-α. The SOLAR2000 v2.22 Lyman-α fluxes span (4.3–4.93) $\times$ 10^{11} photons cm^{-2} s^{-1} during the 9–27 March 1999 period, and (5.16–5.84) $\times$ 10^{11} photons cm^{-2} s^{-1} during the 4 October–4 November 2002 period.

4. Results

4.1. *E* Layer Chemistry

[21] In agreement with previous models of the *E* layer, N_2^+ and O_2^+ are the dominant ions produced from photoionization, yet the dominant *E* layer constituents are NO^+ and O_2^+ [e.g., *Buonsanto et al.*, 1992, 1995; *Titheridge*, 1997, 2000]. Solar EUV and X-ray photons contribute roughly equally to the total photoionization in the *E* layer, while Lyman-α contributes in a minor way by photoionizing NO. The majority of N_2^+ created from photoionization is converted directly to NO^+ via the relatively fast charge-exchange reaction k_8 (see Table 2), while a second-order loss process is reaction k_6, which transfers the charge from N_2 to O_2. Molecular oxygen ions are removed from the *E* layer by dissociative recombination, α_2, or conversion to NO^+, k_5. The conversion of molecular nitrogen and oxygen ions to nitric oxide ions, k_8 and k_5, provides the dominant source of NO^+ in the *E* layer. As the dominant loss for NO^+, α_3, is roughly equivalent to the dissociative recombination rates of O_2^+ and N_2^+, the most important effect of including NO in the model is to change the ionic composition, rather than the electron density. If neutral NO were neglected entirely in *E* layer photochemical calculations (i.e., [NO] = 0), then the modeled electron density would be too large by as much as 10%. The dominant ion would still be NO^+, primarily via reaction k_8, but there would be a larger fraction of O_2^+ ions, thereby resulting in a slower net recombination rate. Atomic oxygen and molecular nitrogen ions play only minor roles (ion mixing ratios $< 10^{-2}$) in the *E* layer.

Table 2. Photoionization, Charge Exchange, and Electron-Ion Recombination Rates

	Reaction	Rate Constant[a]
	Photoionization	
J_1	$O + h\nu \rightarrow O^+ + e^-$	1.9×10^{-9} [b]
J_2	$O_2 + h\nu \rightarrow O_2^+ + e^-$	9.1×10^{-9} [b]
J_3	$N_2 + h\nu \rightarrow N_2^+ + e^-$	3.9×10^{-9} [b]
J_4	$NO + h\nu \rightarrow NO^+ + e^-$	9.2×10^{-7} [b]
	Charge Exchange	
k_1	$O^+ + NO \rightarrow NO^+ + O$	8×10^{-13}
k_2	$O^+ + N_2 \rightarrow NO^+ + N$	1.2×10^{-12}
k_3	$O^+ + O_2 \rightarrow O_2^+ + O$	2.1×10^{-11}
k_4	$O^+ + H \rightarrow H^+ + O$	6.4×10^{-10}
k_5	$O_2^+ + NO \rightarrow NO^+ + O_2$	4.6×10^{-10}
k_6	$N_2^+ + O_2 \rightarrow O_2^+ + N_2$	5×10^{-11}
k_7	$N_2^+ + O \rightarrow O^+ + N_2$	9.8×10^{-12}
k_8	$N_2^+ + O \rightarrow NO^+ + N$	1.3×10^{-10}
k_9	$N_2^+ + NO \rightarrow NO^+ + N_2$	4.1×10^{-10}
	Recombination	
α_1	$N_2^+ + e^- \rightarrow N + N$	$2.2 \times 10^{-7} (300/T)^{0.39}$
α_2	$O_2^+ + e^- \rightarrow O + O$	$1.95 \times 10^{-7} (300/T)^{0.7}$
α_3	$NO^+ + e^- \rightarrow N + O$	$4.0 \times 10^{-7} (300/T)^{0.5}$

[a] Units are s^{-1} for J_i, cm^3 s^{-1} for k_i and α_i.
[b] Units are cm^6 s^{-1}. Computed at Bermuda for 110 km, 1200 LT, on 9 Mar 1999.

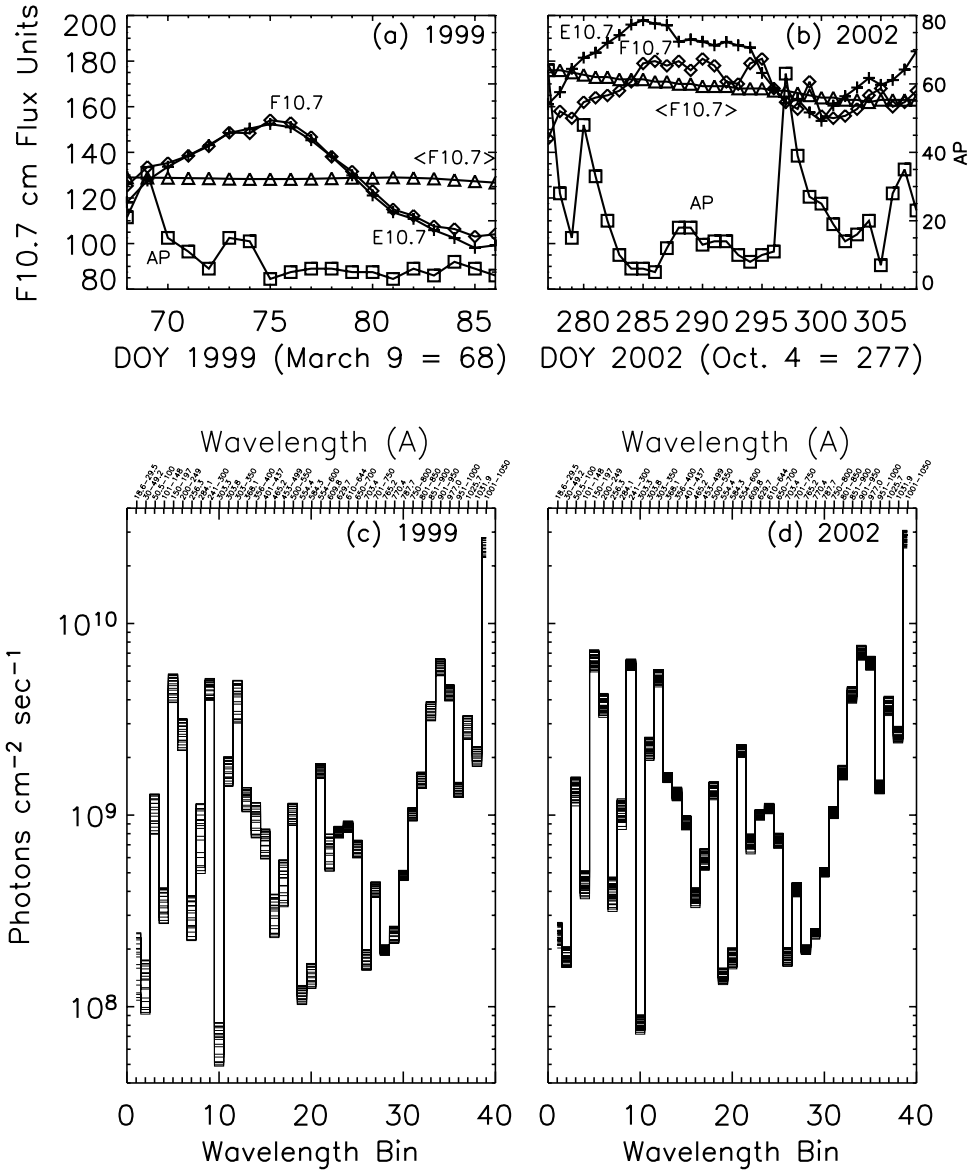

Figure 6. Solar inputs used in this study for the (a) 9–27 March 1999 and (b) 4 October–4 November 2002 periods. The term E10.7 in Figures 6a and 6b comes from the empirical model of solar flux, SOLAR2000, and is derived from the EUV and X-ray portion of the spectrum that is responsible for photoionization in the ionosphere [see *Tobiska et al.*, 2000]. It is given here in order to compare with F10.7, which, along with ⟨F10.7⟩ and AP, drives the NRLMSISE-00 model. These terms, F10.7, ⟨F10.7⟩, and AP, have their usual representations of the 10.7 cm solar radio flux, an 81 day running mean of that radio flux, and a measure of the daily magnetic activity, respectively. (c, d) Photon flux as a function of wavelength over the 19 days in 1999 (Figure 6c) and 32 days in 2002 (Figure 6d), as given by SOLAR2000 v2.22.

[22] Examples of the modeled noontime *E* layer are given in Figure 7, with the ion constituents labeled (Figures 7a and 7b), and the electron density shown as the solid curve. There is a significant difference in the calculated NO^+/O_2^+ ion ratios for Millstone Hill (42.6° latitude) and Svalbard (78.2° latitude), mostly owing to the larger NO densities found in the polar regions. Daily modeled electron altitude profiles at Millstone Hill and Svalbard are given in Figures 7c and 7d, and should be compared with the 100–150 km altitude regions of Figures 1 and 2, respectively. The modeled profiles provide a good match for midlatitudes, and capture the observed behavior at Millstone Hill, as well as the high variability at Svalbard.

4.2. Comparison Between Model and Data

[23] The photochemical model of the *E* layer described above performs very well in matching measurements of electron density near noon at a variety of latitudes, longitudes, and time periods. Comparisons between daily modeled and observed N_mE profiles are given in Figure 3 for a

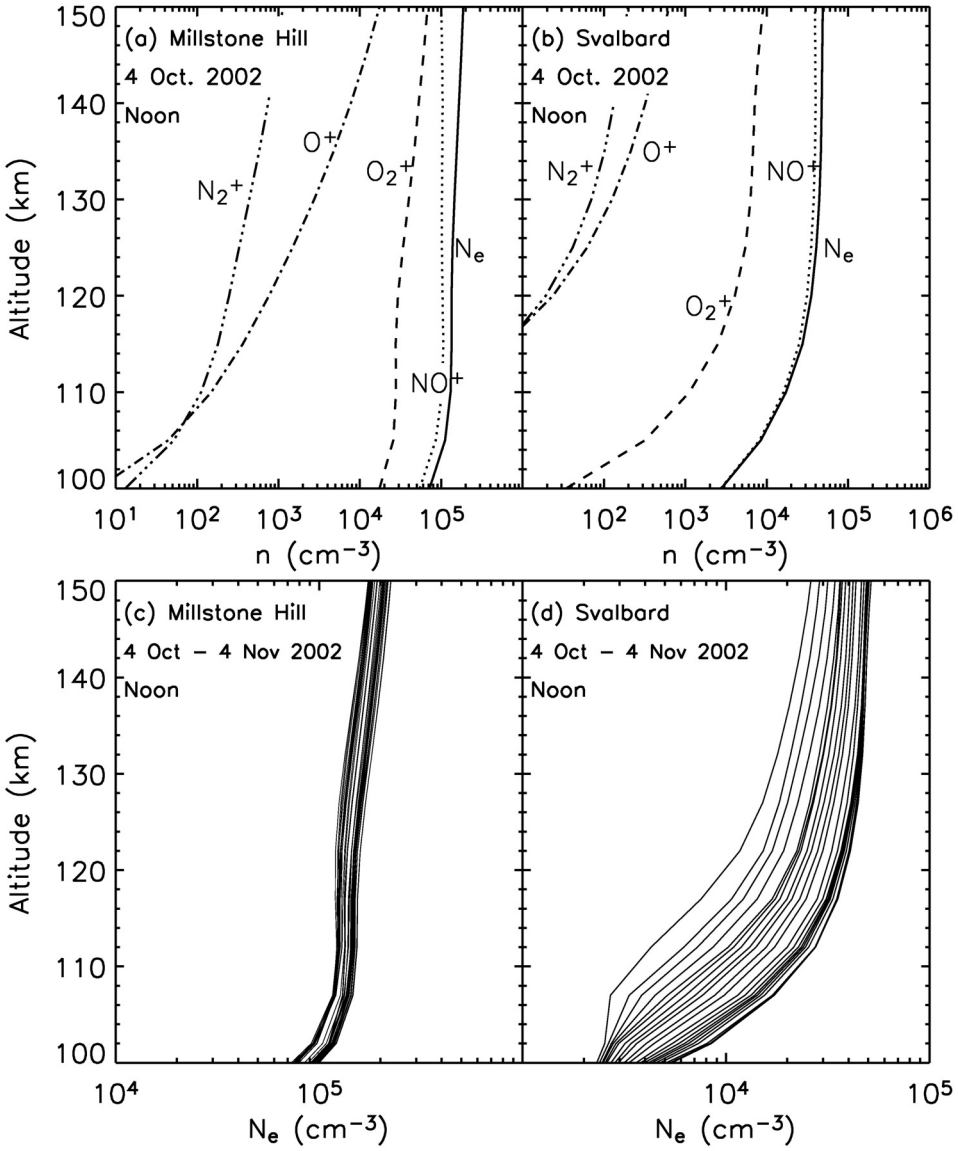

Figure 7. An example of modeled ion altitude profiles for 1200 LT on 4 October 2002 at (a) Millstone Hill and (b) Svalbard. The ion species are labeled, and the electron density is the sum of the ion species, given as a solid curve. Also plotted are the modeled electron density altitude profiles for the 4 October–4 November 2002 period at (c) Millstone Hill and (d) Svalbard. These scatterplots should be compared with the 100–150 km altitude regions in Figures 1 and 2.

subauroral station, Millstone Hill, and Figure 4 for a lower midlatitude station, Eglin AFB, during both the 1999 and the 2002 time periods. The good agreement displayed in Figures 3 and 4 is typical of the rest of the midlatitude stations. As it is most fruitful to study the variability of a process during its most stable local time period, this work focuses on noontime day-to-day variability. The diurnal profiles of N_mE in Figures 3 and 4 are given in order to fully appreciate the context of the *E* layer data; however, in the context of noontime variability, agreement between the model and the observations near dawn and dusk is not necessary. Therefore a simple Chapman approximation was used to calculate production at large solar zenith angles.

[24] There is too much data to show comparisons with the model at all stations. Instead, the extreme noontime N_mE values (i.e., the minimum and maximum value of N_mE over the course of each time period), the mean N_mE values, and the standard deviations about the mean are extracted from each observation and each modeled prediction and summarized in Figures 8 and 9. In terms of absolute values of N_mE (Figure 8), it is clear that the model has a smaller range of peak electron density values during both time periods and at all stations, and generally demonstrates a lower mean N_mE. This does not necessarily imply that the modeled standard deviations are smaller, however. Calculated standard deviations from 19 days (9–27 March 1999) and from 32 days (4 October–4 November 2002) are given in Figure 9. The 1999 period demonstrates more variability than the 2002 period, both from model calculations and observations. It is worth noting that there is noticeably more solar variability

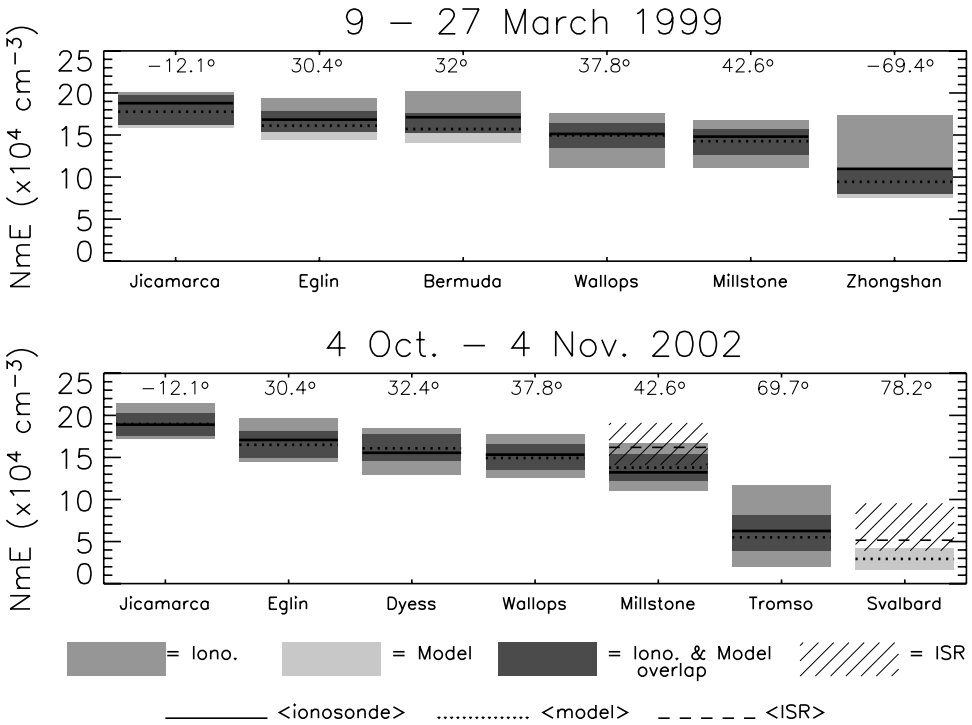

Figure 8. A comparison between the modeled and observed ranges of noontime *E* layer electron density for (top) 9–27 March 1999 and (bottom) 4 October–4 November 2002. All observations are made by ionosondes, except for the two ISR measurements, which are represented by diagonal hash marks in the bottom panel. Dark shaded boxes correspond to regions where the ionosonde measurement and model prediction overlap; otherwise, modeled ranges are given by light shaded boxes and observed ranges by medium shaded boxes. Mean N_mE values for the period are given as solid (ionosonde), dotted (model), and dashed (ISR) lines. Latitudes are given above each station.

in the SOLAR2000 v2.22 irradiances for 1999, especially in the soft X-ray and EUV portion of the solar spectrum (Figure 6). Modeled and observed standard deviations agree quite well at equatorial and midlatitudes, and observed variabilities are all above any inherent instrumental variability due to measurement precision (±0.05 MHz). Exceptions to that good agreement, e.g., at Dyess in 2002, might be explained by the large amount of magnetic activity during the 2002 period inducing neutral atmospheric variations that were not adequately portrayed by MSIS. At auroral latitudes, the differences between modeled and observed variability can be attributed to auroral ionization processes, the consequences of which are discussed below.

4.3. Contributions to *E* Layer Variability

[25] The good agreement between modeled and observed N_mE densities and their variabilities near noon displayed in Figures 8 and 9 gives confidence that the model has reasonable accuracy for nonstorm/nonauroral conditions. At this point, the advantages of a theoretical model can be utilized to determine the dominant sources of variability. There are four model inputs that contribute to some degree to the total variability of the *E* layer electron densities: (1) change of solar declination over the time period studied, (2) NO density variations, (3) neutral atmospheric variations (all non-NO constituents), and (4) solar flux variations. *E* layer densities were calculated within the model by allowing only one of the four sources to vary individually. Thus for a particular station and time period, there were five model runs, one for each different source of variability and one where all sources were allowed to vary together. The results of these calculations are summarized in Table 1 and Figures 8 and 9. Three interesting points arise from this analysis: (1) solar flux is the dominant source of variability in the *E* layer at middle and low latitude, (2) changes in solar declination are a secondary source variability at midlatitude, and a dominant source at high latitude, and (3) the net variability in N_mE is not a simple combination of parameters, such as the sum of the squares of the variability, but rather there is a feedback between the different sources. These points can be verified from the values in Table 1, where the largest contributions to *E* layer variability come from changes in the solar flux (column d) and the solar declination (column a).

[26] The first point can be understood to arise from the fact that ionization in the mid- and low-latitude *E* layer is dominated by solar photons, and that all of the other sources of variability described above are secondary effects that act only as a result of photoionization. It is clear that the second point, a changing solar declination, would be a source of variability that is more important at high latitudes, but it is not obvious a priori how it would compare with other sources of variability. The model calculations show that it can be quite important, even at midlatitudes for a month of quiet solar conditions. Additionally, this source becomes a stronger source of variability as the period of study becomes

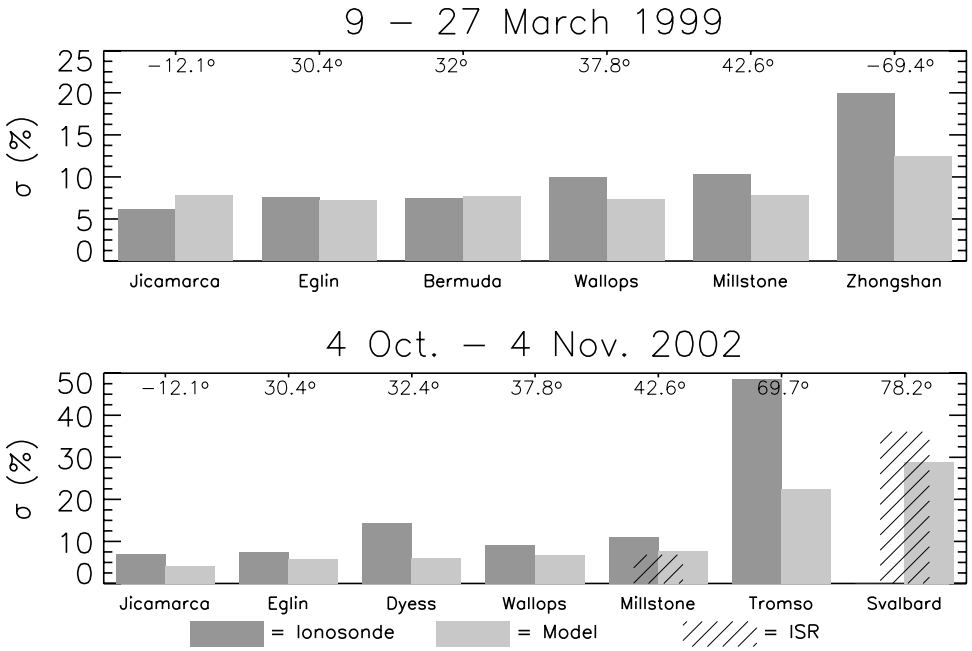

Figure 9. Comparison between modeled and observed standard deviations of mean N_mE at noon for (top) 9–27 March 1999 and (bottom) 4 October–4 November 2002. Note that the scales are different for the two periods. Ionosonde measurements are given by dark shaded boxes, modeled standard deviations by light shaded boxes, and ISR measurements by the angled hash marks. Latitudes are given above each station.

longer. Understanding the third point, how different sources of variability are combined, involves multistage coupling effects. For instance, a day with high solar activity would also likely be a day with high NO densities, as solar soft X rays are the dominant source of NO production at middle to low latitudes [*Bailey et al.*, 2002; *Barth and Bailey*, 2004]. Larger NO densities lead to smaller electron densities, primarily due to the fact that NO removes N_2^+ ions from the *E* layer, and NO^+ has a faster recombination rate (see Table 2) [*Titheridge*, 1997]. Thus a single source of variability (higher solar flux) changes both production and loss of electron densities, and this mitigation reduces the modeled variability when all sources are considered together.

[27] For stations in the auroral regions (i.e., Svalbard, Tromso, and Zhongshan in this study), the model only accounts for ∼45–67% of the extremes of N_mE observed, and ∼50–80% of the variability observed (Figures 8 and 9). The remaining electron production that leads to a wider range of N_mE and a larger day-to-day variability is most likely due to auroral sources of ionization, which are not modeled here. Ion and electron precipitation can also lead to increased production of NO in the thermosphere; that behavior is captured in this study by including NO measurements from the SNOE satellite. Thus for days of high auroral activity, the model is using the properly enhanced NO densities, but the electron production in those regions is deficient. This deficiency is slightly compounded by the fact that larger NO densities lead to smaller electron densities in the *E* layer. Since the other important *E* layer effect of auroral precipitation, enhanced NO, is already included in the model, the primary effect of increased ionization gives the same result as an increased photon flux. In other words, the auroral contribution to the net variability can be estimated by increasing the photon flux until the ranges of N_mE from the model and the observations overlap. The result of such an estimate is that auroral sources account for ∼30% of the variability at Zhongshan in 1999, ∼25% of the variability of Svalbard in 2002, and ∼40% of the variability of Tromso in 2002 (Figure 9).

5. Summary

[28] A photochemical one-dimensional model of the *E* layer has been constructed in order to study the sources of variability in the best-documented photochemical ionospheric layer in the solar system, the terrestrial *E* layer. Comparisons between model calculations and observations (ionosonde and ISR) for two different time periods (9–27 March 1999 and 4 October–4 November 2002), and at many different latitudes show good agreement both in magnitude (Figure 8) and standard deviation (Figure 9). The photochemical model makes use of other models and parameterizations in order to characterize the atmosphere and solar flux: the SOLAR2000 (v2.22) model of the Sun's irradiance [*Tobiska et al.*, 2000; *Tobiska*, 2004] and NRLMSISE-00 [*Picone et al.*, 2002], for the neutral atmosphere. Electron density observations are gathered from the SPIDR and Madrigal databases for ionosonde and ISR measurements, respectively. Neutral NO profiles are obtained from the SNOE satellite's measurements [*Barth et al.*, 2003].

[29] Secondary ionization is an extremely important process in the *E* layer; by including secondary ionization sources the calculated electron density is nearly doubled. Calculations made with the most recent version of

SOLAR2000 (v2) produce *E* layer electron densities roughly a factor of 2 smaller than calculations using prior solar flux models (e.g., SOLAR2000 v1), indicating that there may be uncertainty remaining in either primary ionization rates (e.g., solar flux, photoionization cross sections, especially at low wavelength, and neutral atmospheric densities), or the secondary ionization rates, or both. However, the new version of SOLAR2000 may itself be controversial.

[30] The dominant source of variability in the mid- and low-latitude *E* layer is shown to be solar photons directly ionizing the atmosphere, rather than those photons altering the constituent densities within the atmosphere. In most cases the geometrical effect of a shift in the solar declination over a period of weeks is the secondary source of *E* layer variability. For polar latitudes, and/or longer time periods, this geometric effect can become the dominant source of variability. From the photochemical model calculations, it is estimated that auroral sources account for ~30% of the total day-to-day variability at polar stations on average. These results support the notion that the *E* layer can be generally well reproduced with a relatively simple photochemical model.

[31] **Acknowledgments.** We thank John Holt (Millstone Hill) and Tony Van Eyken (EISCAT) for making us aware of the ISR "long runs" in 2002 and for making these data sets available through the Madrigal Database. EISCAT is an international association supported by Finland (SA), France (CNRS), Germany (MPG), Japan (NIPR), Norway (NFR), Sweden (VR), and the United Kingdom (PPARC). We acknowledge the SPIDR database for the ionosonde observations used in this study. Finally, SOLAR2000 Research Grade historical irradiances are provided courtesy of W. Kent Tobiska and SpaceWx.com. These historical irradiances have been developed with funding from NASA UARS, TIMED, and SOHO missions. This work was supported by the NSF Aeronomy Program and the NASA Graduate Student Researchers Program.

[32] Arthur Richmond thanks Henry Rishbeth and another reviewer for their assistance in evaluating this paper.

References

Bailey, S. M., C. A. Barth, and S. C. Solomon (2002), A model of nitric oxide in the lower thermosphere, *J. Geophys. Res.*, *107*(A8), 1205, doi:10.1029/2001JA000258.

Barth, C. A., and S. M. Bailey (2004), Comparison of a thermospheric photochemical model with Student Nitric Oxide Explorer (SNOE) observations of nitric oxide, *J. Geophys. Res.*, *109*, A03304, doi:10.1029/2003JA010227.

Barth, C. A., W. K. Tobiska, D. E. Siskind, and D. D. Cleary (1988), Solar-terrestrial coupling: Low-latitude thermospheric nitric oxide, *Geophys. Res. Lett.*, *15*, 92–94.

Barth, C. A., K. D. Mankoff, S. M. Bailey, and S. C. Solomon (2003), Global observations of nitric oxide in the thermosphere, *J. Geophys. Res.*, *108*(A1), 1027, doi:10.1029/2002JA009458.

Barth, C. A., D. N. Baker, and S. M. Bailey (2004), Seasonal variation of auroral electron precipitation, *Geophys. Res. Lett.*, *31*, L04809, doi:10.1029/2003GL018892.

Buonsanto, M. J., S. C. Solomon, and W. K. Tobiska (1992), Comparison of measured and modeled solar EUV flux and its effect on the E-F1 region ionosphere, *J. Geophys. Res.*, *97*, 10,513–10,524.

Buonsanto, M. J., P. G. Richards, W. K. Tobiska, S. C. Solomon, Y.-K. Tung, and J. A. Fennelly (1995), Ionospheric electron densities calculated using different EUV flux models and cross sections: Comparison with radar data, *J. Geophys. Res.*, *100*, 14,569–14,580.

Grebowsky, J. M., R. A. Goldberg, and W. D. Pesnell (1998), Do meteor showers significantly perturb the ionosphere?, *J. Atmos. Sol. Terr. Phys.*, *60*, 607–615.

Lilensten, J., W. Kofman, J. Wisemberg, E. S. Oran, and C. R. Devore (1989), Ionization efficiency due to primary and secondary photoelectrons: A numerical model, *Ann. Geophys.*, *7*, 83–90.

Marsh, D. R., S. C. Solomon, and A. E. Reynolds (2004), Empirical model of nitric oxide in the lower thermosphere, *J. Geophys. Res.*, *109*, A07301, doi:10.1029/2003JA010199.

Martinis, C. R., J. K. Wilson, and M. J. Mendillo (2003), Modeling day-to-day ionospheric variability on Mars, *J. Geophys. Res.*, *108*(A10), 1383, doi:10.1029/2003JA009973.

Mendillo, M., S. Smith, J. Wroten, H. Rishbeth, and D. Hinson (2003), Simultaneous ionospheric variability on Earth and Mars, *J. Geophys. Res.*, *108*(A12), 1432, doi:10.1029/2003JA009961.

Moore, L. E., M. Mendillo, I. C. F. Müller-Wodarg, and D. L. Murr (2004), Modeling of global variations and ring shadowing in Saturn's ionosphere, *Icarus*, *172*, 503–520.

Picone, J. M., A. E. Hedin, D. P. Drob, and A. C. Aikin (2002), NRLMSISE-00 empirical model of the atmosphere: Statistical comparisons and scientific issues, *J. Geophys. Res.*, *107*(A12), 1468, doi:10.1029/2002JA009430.

Richards, P. G., and D. G. Torr (1988), Ratios of photoelectron to EUV ionization rates for aeronomic studies, *J. Geophys. Res.*, *93*, 4060–4066.

Richards, P. G., J. A. Fennelly, and D. G. Torr (1994), EUVAC: A solar EUV flux model for aeronomic calculations, *J. Geophys. Res.*, *99*, 8981–8992.

Rishbeth, H., and M. Mendillo (2004), Ionospheric layers of Earth and Mars, *Planet. Space Sci.*, *52*, 849–852.

Russell, J. M., III, L. L. Gordley, L. E. Deaver, R. E. Thompson, and J. H. Park (1994), An overview of the halogen occultation experiment (HALOE) and preliminary results, *Adv. Space Res.*, *14*(9), 13–20.

Schunk, R. W., and A. F. Nagy (2000), *Ionospheres: Physics, Plasma Physics, and Chemistry*, Cambridge Univ. Press, New York.

Siskind, D. E., C. A. Barth, and R. G. Roble (1989a), The response of thermospheric nitric oxide to an auroral storm: 1. Low and middle latitudes, *J. Geophys. Res.*, *94*, 16,885–16,898.

Siskind, D. E., C. A. Barth, D. S. Evans, and R. G. Roble (1989b), The response of thermospheric nitric oxide to an auroral storm: II. Auroral latitudes, *J. Geophys. Res.*, *94*, 16,899–16,911.

Siskind, D. E., C. A. Barth, and J. M. Russell III (1998), A climatology of nitric oxide in the mesosphere and thermosphere, *Adv. Space Res.*, *21*, 1353–1362.

Solomon, S. C., and V. J. Abreu (1989), The 630 nm dayglow, *J. Geophys. Res.*, *94*, 6817–6824.

Solomon, S. C., P. B. Hays, and V. J. Abreu (1988), The auroral 6300 Å emission: Observations and modeling, *J. Geophys. Res.*, *93*, 9867–9882.

Solomon, S. C., et al. (1996), The Student Nitric Oxide Explorer, *Proc. SPIE*, *2810*, 1–12.

Solomon, S. C., C. A. Barth, and S. M. Bailey (1999), Auroral production of nitric oxide measured by the SNOE satellite, *Geophys. Res. Lett.*, *26*, 1259–1262.

Titheridge, J. E. (1996), Direct allowance for the effect of photoelectrons in ionospheric modeling, *J. Geophys. Res.*, *101*, 357–369.

Titheridge, J. E. (1997), Model results for the ionospheric E region: Solar and seasonal, *Ann. Geophys.*, *15*, 63–78.

Titheridge, J. E. (2000), Modelling the peak of the ionospheric E-layer, *J. Atmos. Sol. Terr. Phys.*, *62*, 93–114.

Tobiska, W. K. (2004), SOLAR2000 irradiances for climate change research, aeronomy and space system engineering, *Adv. Space Res.*, *34*, 1736–1746.

Tobiska, W. K., T. Woods, F. Eparvier, R. Viereck, L. Floyd, D. Bouwer, G. Rottman, and O. R. White (2000), The SOLAR2000 empirical solar irradiance model and forecast tool, *J. Atmos. Sol. Terr. Phys.*, *62*, 1233–1250.

S. Bailey, Geophysical Institute, University of Alaska Fairbanks, Fairbanks, AK 99775, USA.

C. Martinis, M. Mendillo, and L. Moore, Center for Space Physics, Boston University, 725 Commonwealth Avenue, Boston, MA 02215, USA. (moore@bu.edu)